ORIGINAL ARTICLE

Is percutaneous fixation of the superior pubic ramus possible in all types of pelvis?

Harun Altınayak, M.D.,[1] Orhan Balta, M.D.[2]

[1]Department of Orthopaedics and Traumatology, Samsun Training and Research Hospital, Samsun-*Türkiye*
[2]Department of Orthopaedics and Traumatology, Tokat Gaziosmanpaşa University Faculty of Medicine, Tokat-*Türkiye*

ABSTRACT

BACKGROUND: The impact of pelvis type on percutaneous fixation of the superior pubic ramus was investigated in this study.

METHODS: One hundred fifty pelvic CTs (female/male: 75/75) without anatomical changes in the pelvis were studied. Pelvis CT examinations with 1mm section width, pelvis typing, anterior obturator oblique, and inlet section images were created using the MPR and 3D imaging mode of the imaging system. In these images, whether a linear corridor could be obtained for the superior pubic ramus, corridor width, length, and angle values in the transverse and sagittal planes were measured in pelvic CT where linear corridor could be obtained.

RESULTS: In 11 samples (7.3 %) (group 1), no linear corridor for the superior pubic ramus could be obtained in any way. All pelvis types in this group were gynecoid, and all belonged to female patients. A linear corridor in the superior pubic ramus could be easily obtained in all pelvic CTs with Android pelvic type. The superior pubic ramus was 8.2±1.8 mm in width and 116.7±12.8 mm in length. The corridor width was measured below 5 mm in 20 (13.3%) pelvic CT images (group 2). Corridor width showed a statistically significant difference depending on the pelvic type and gender.

CONCLUSION: The pelvic type is a determinat factor for the fixation of the percutaneous superior pubic ramus. For this reason, pelvic typing using MPR and 3D imaging mode in preoperative CT examination; is effective in surgical planning, implant, and surgical position selection.

Keywords: 3D imaging; MPR; pelvis CT; percutan screw fixation; superior pubic ramus.

INTRODUCTION

The growing frequency of high-energy trauma due to technological developments and greater life expectancy in the elderly population has increased the incidence of pelvis-acetabulum fractures.[1–3] Complex fracture patterns and associated injuries in high-energy trauma patients, poor bone quality in elderly trauma patients, complex pelvic and soft tissue anatomy, and the potential for comorbid diseases make the treatment of these injuries difficult. The desire to avoid the morbidity of open surgery and technical and conceptual advances in intraoperative image acquisition and interpretation have led to the development of minimally invasive fixation.[4–7] Percutaneous pelvic screw insertion is a technically demanding procedure that requires the surgeon to fully understand the pelvic osseous fixation pathways and their fluoroscopic imaging.[8]

Superior pubic ramus fractures are a common fracture type in the pelvis and are typically associated with pelvic ring damage. Superior pubic ramus fractures occur in the parasymphyseal, midramus, or adjacent to the lower anterior acetabular column and wall.[9] Although percutaneous insertion of long screws into the superior pubic ramus has become an important component of the minimally invasive orthopedic treatment of pelvic fractures, no consensus has been found. Nonetheless, clinical, anatomical, and imaging studies have been conducted to determine how screw diameter, screw

Cite this article as: Altınayak H, Balta O. Is percutaneous fixation of the superior pubic ramus possible in all types of pelvis?. Ulus Travma Acil Cerrahi Derg 2023;29:419-429.

Address for correspondence: Harun Altınayak, M.D.
Samsun Eğitim ve Araştırma Hastanesi, Ortopedi ve Travmatoloji Kliniği, Samsun
Tel: +90 362 - 311 150 0 E-mail: harun240507@gmail.com

Ulus Travma Acil Cerrahi Derg 2023;29(3):419-429 DOI: 10.14744/tjtes.2023.54545 Submitted: 22.11.2022 Revised: 11.01.2023 Accepted: 20.02.2023

length, screw orientation axis, and gender differences affect these components.[9–18] However, no study in the literature has examined whether pelvic type affects the diameter and length of the superior pubic ramus or the fixation of percutaneous superior pubic ramus fractures. For this reason, the present study used pelvic computed tomography (CT) to determine pelvic type and investigated how the pubic ramus affects diameter, length, and direction.

MATERIALS AND METHODS

This study used 150 pelvic CT images (75 women; 75 men) to evaluate the pubic ramus (95% confidence interval (1-α); 95.3% test power (1-β); and d=0.676; the number of samples is set to 98).[19] After obtaining approval from the local ethics committee, the pelvic CTs (with slice widths of 1 mm) of patients between the ages of 16–100 years were examined at the diagnostic imaging center of our hospital. Images with impaired pelvic anatomy, such as those with recent or previous pelvis-acetabulum fractures, primary and metastatic tumoral formations in the pelvis, and findings indicative of surgical intervention, developmental hip dysplasia, and total hip arthroplasty, were excluded from the study. CT images were evaluated using multiplanar reformation (MPR) and the 3D imaging mode of the imaging system (Sectra Workstation IDS7 Version 21.2.13.6313 © 2019 Sectra AB, Linköping, Sweden). In the MPR imaging mode, CT sections were constructed to create anterior obturator oblique (AOO) and inlet images for the evaluation of the superior pubic ramus (Fig. 1).

In these sections, it was determined whether a linear intramedullary osseous fixation corridor described for the pubic arm was obtained from the pubic tubercle to the supraacetabular region for fixation of the superior pubic ramus (Fig. 2).[12,20] In the CT images obtained from the linear corridor, the widths and lengths of the columns in both planes were

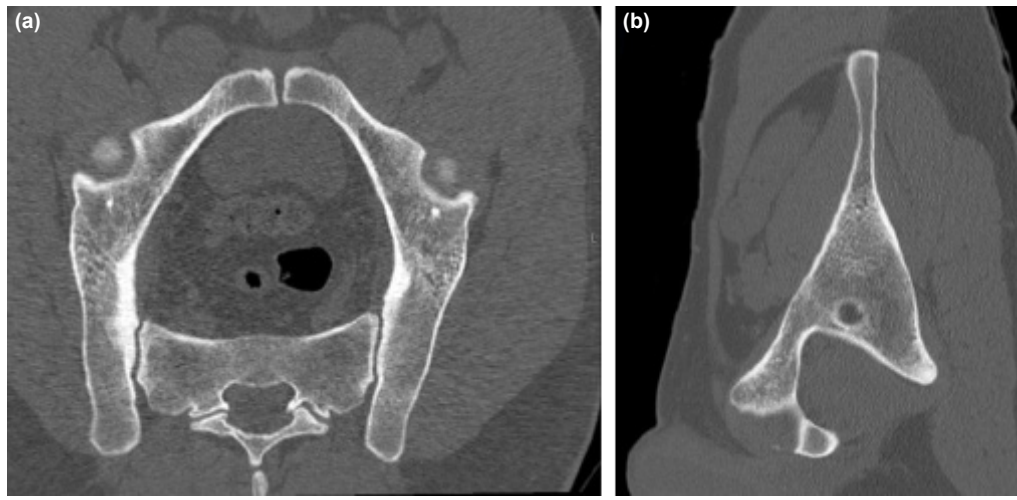

Figure 1. Obtained using multiplanar reformation mod **(a)** Inlet section view, **(b)** Anterior obdurator oblique (AOO) section view.

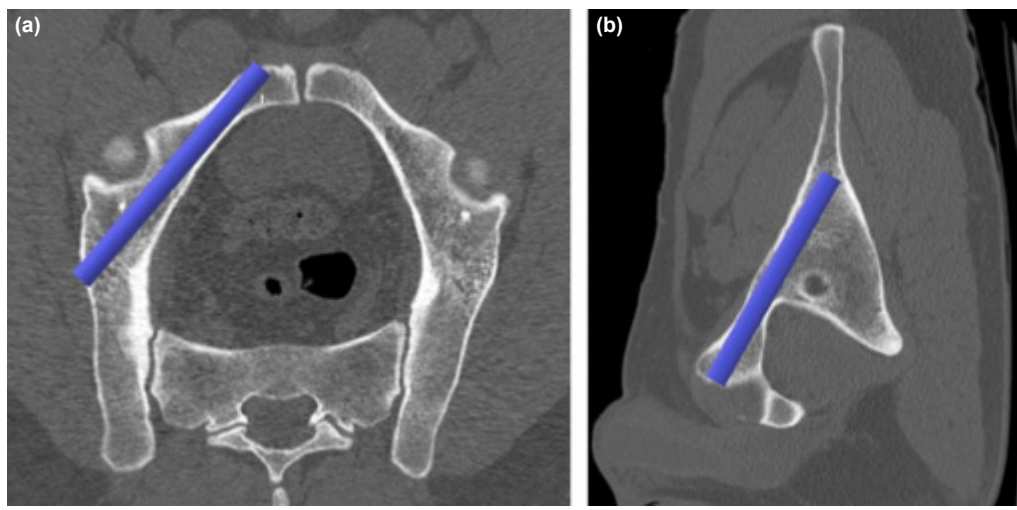

Figure 2. Linear intramedullary osseous fixation corridors in cross-sectional images. **(a)** View of linear superior pubic ramus in inlet cross-sectional view, **(b)** View of linear superior pubic ramus in anterior obdurator oblique cross-sectional view.

measured. The angles in the coronal and sagittal planes required to obtain a linear corridor in the same cross-sectional images were made (Fig. 3). The widths and lengths of the medial and lateral corridors were measured in pelvic CT examinations where no linear corridor could be obtained (Fig. 4). In the width and length measurement values of the corridors, the shorter of the cross-sectional images was used. For pelvic typing, which is the primary subject of our study's hypothesis, pelvic typing was performed on all CT images in MPR and the 3D imaging mode using the measurement techniques described in the literature.[21–23]

Pelvis Typing

Pelvis CT images were analyzed using measurement techniques described in the literature.[21–23] Pelvimetry was performed using MPR and 3D images. The largest transverse diameter, anteroposterior diameter, interspinous-intertuberous distance, the subpubic arch, the sacrosiatic notch, the ischial spines, and the sacral slope were evaluated using two different approaches in each dataset.

First, 2D multiplane reconstructions were performed on 1 mm slices. To measure the transverse entrance diameter, the plane was set in a para-axial position so that the upper edge of the pelvic inlet was displayed in an oval shape (Fig. 5a). A para-axial plane was chosen to measure the intertuberous distance to show both ischial tuberosities (Fig. 5b). To measure mid-pelvic distances, i.e., the interspinous distance at the level of the ischial spines, the plane was adjusted to show the lower inner border of the symphysis and both ischial vertebrae (Fig. 5c). The midsagittal plane was used to measure the anteroposterior diameter from the sacral promontorium to the upper inner border of the symphysis (Fig. 5d). The fact that the symphysis was composed of collagen and had a smaller diameter than the adjacent bone generally required minimal shift to the slight paramedian plane.

In another approach, 3D volumetric rendered images of the same 1mm slices were evaluated with a technique that implies measurements in standard cranial, posterior, and lateral views: the transverse diameter of the inner pelvis was measured on the 3D view from a cranial view (Fig. 5e). In the posterior view, the interspinous distance was measured as the shortest distance between both ischial spines, and the intertuberous distance was measured as the widest distance between the ischial tuberosity (Fig. 5f). Then, the data set

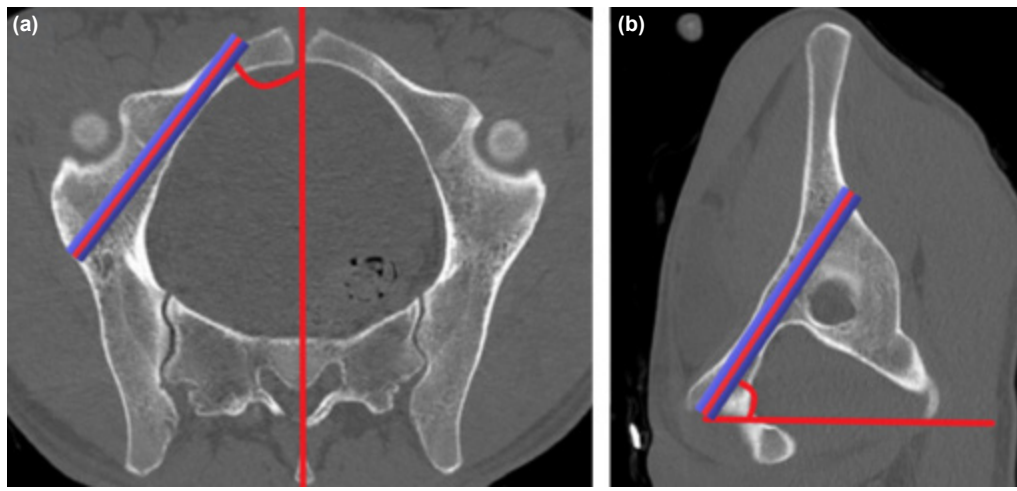

Figure 3. Linear superior pubic corridor **(a)** angulation in the coronal plane from medial to lateral, **(b)** angulation in the sagittal plane in the caudocranial direction.

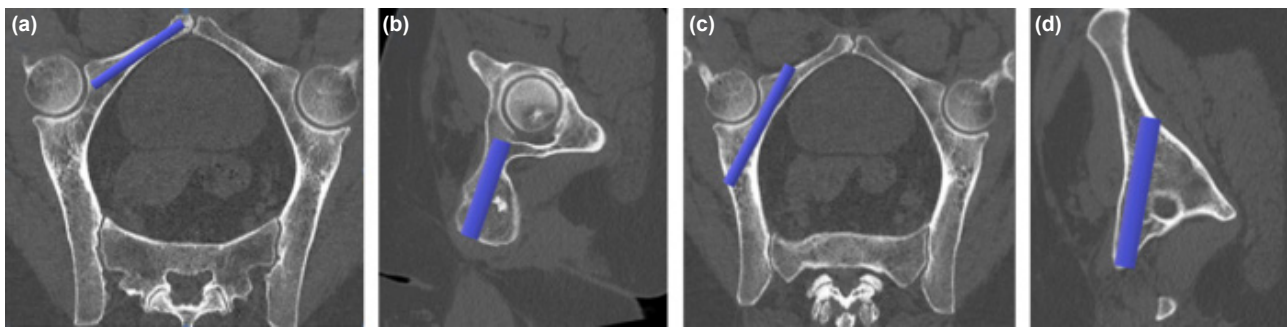

Figure 4. Medial and lateral intramedullary osseous fixation corridors in CT examinations where a linear corridor cannot be created. **(a)** Medial corridor view in inlet cross-section view, **(b)** medial corridor view in AOO cross-section view, **(c)** lateral corridor view in inlet cross-section view, **(d)** lateral corridor view in AOO cross-section view. (AOO: Anterior obdurator oblique).

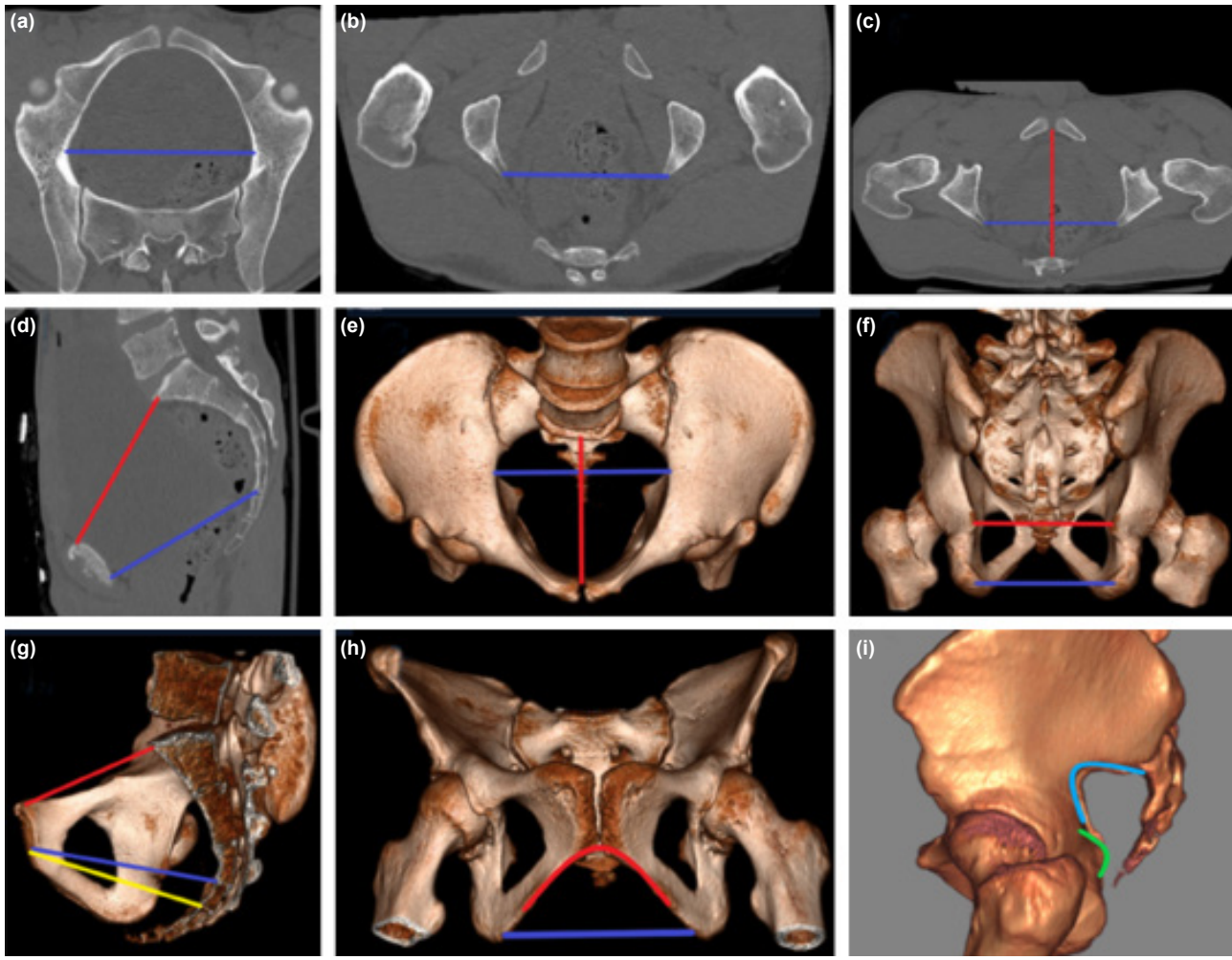

Figure 5. Pelvis typing; **(a)** Para-axial reconstruction showing the pelvic inlet. Widest transverse diameter of inlet view. **(b)** Axial slice showing ischial tuberosities and the corresponding measurement. **(c)** Para-axial reconstruction showing ischial spines, the caudal end of the symphysis and the sacrum so that interspinal distance and sagittal midpelvic diameter can be measured. **(d)** Sagittal reconstruction showing the symphysis and the sacrum. Red line: anteroposterior diameter, blue line: sagittal outlet diameter. **(e)** Volume-rendered reconstruction in a superior–anterior view. Blue line: Widest transverse diameter, Red line: anteroposterior diameter. **(f)** Posterior view, with lines showing interspinous (red) and intertuberous (blue) measurements. **(g)** Right lateral view of the pelvis split in half in a sagittal plane. Lines indicate anteroposterior diameter (red), sagittal midpelvic diameter (blue) and sagittal outlet (yellow). **(h)** Subpubik arc (red) and transvers diamater of outlet (blue). **(i)** Sacrosciatic notch (blue), ischial spine (green).

was cut in the midsagittal direction, and sagittal measurements were obtained on a lateral view. These included the anteroposterior diameter as the shortest distance between promontory and symphysis and sacral slope (Fig. 5g). In addition, the outlet's subpubic arc, transverse diameter, sacrosiatic notch, and ischial spines were evaluated (Fig. 5h-i). After the pelvic typing process, grouping was done in four main pelvis types. Some pelvis types did not fit the main group exactly. These were added to the closest main pelvis group. The four main pelvic types are gynecoid, android, anthropoid, and platypelloid. The gynecoid form has a rounded or slightly transverse oval-shaped pelvic edge. It has a wide subpubic arch, and the sacrum is curved posteriorly. The android form has a "pear-shaped" edge with the largest transverse diameter and is closer to the sacrum than the groin. The subpubic arch is narrow, the sacrum is anteriorly curved, and the cavity is funnel-shaped with prominent ischial spines. Anthropoid, despite its name, refers to a more ape-like shape; here, the anteroposterior diameter at the rim is significantly larger than the lateral, giving a long, narrow oval shape. Finally, the platypelloid form is where the lateral diameter at the edge is significantly greater than the AP, giving it a flat or transverse oval form.

Statistical Analysis

Data were analyzed with IBM SPSS V23. Conformity to the normal distribution was evaluated using the Shapiro-Wilk test. The chi-square test was used to compare categorical variables according to groups. The Mann-Whitney U test was used for non-normally distributed data in the comparison of quantitative variables according to the paired groups, and the independent two-sample t-test was used for the comparison

of normally distributed data. A paired two-sample t-test was used to compare normally distributed data according to in-group corridors, and the Wilcoxon test was used to compare non-normally distributed data. Analysis results were presented as mean±standard deviation and median (minimum-maximum) for quantitative data and frequency (percent) for categorical data. The significance level was taken as $p<0.05$.

RESULTS

In 11 (7.3%) of the 150 examined pelvic CT images, no linear corridor for the superior pubic ramus could be obtained in any way. To obtain a corridor in 20 (13.3%) pelvic CT images, the retrograde starting point required an increased orientation angle in the caudocranial direction within the sagittal plane and a more distally oriented angle in the parasymphyseal region. All 31 of these pelvic CT images were from female patients. After the first evaluation, 11 pelvic CT images that could not obtain a linear corridor within the superior pubic ramus in any way were included in group 1; more distal retrograde starting points that were needed to obtain a linear corridor in the parasymphyseal region and 20 pelvic CT images that required an increased angle in the caudocranial direction of the sagittal plane were included in group 2; and easily superior pubic starting points and the 119 pelvic CT images that could obtain a linear corridor in the arm were included in group 3.

The mean age of the study's sample was 53.4±21.9 years (min: 16–max: 101). The average age was 52.8±21.8 years in males and 54.1±22.1 years in females. No statistical differences were found in the mean ages of the patients according to gender (p=0.731) (Table 1).

In the pelvis typing that was conducted according to gender, there were 69 (92%) android, 4 (5.3%) platypelloid, and 2 (2.7%) anthropoid pelvis types in the CT images of male patients, and 38 (50.7%) gynecoid, 23 (30.7%) android, 8 (10.7%) platypelloid, and 6 (8%) anthropoid pelvis types in the CT images of female patients. There was a statistically significant difference between the distributions of the pelvis type according to gender ($p<0.001$) (Table 2). In the pelvis typing, the linear corridor could not be obtained. Furthermore, the pelvis type was gynecoid in all CT images for group 1. There were 15 (75%) gynecoid, 4 (20%) platypelloid, and 1 (5%) anthropoid pelvic types in the CT images of group 2. The CT images of group 3 showed 92 (77.3%) android, 12 (10.1%) gynecoid, 8 (6.7%) platypelloid, and 7 (5.9 %) anthropoid pelvis types. While a linear corridor could be obtained in all android pelvis types (100%), either a linear corridor could

Table 1. Comparison of the ages of the patients according to their gender

	Mean±SD	Mean (Min-Max)	Test statistics	p
Male	52.8±21.8	57.0 (18.0–90.0)	t=-0.345	0.731
Female	54.1±22.1	58.0 (18.0–101.0)		
Total	53.4±21.9	57.5 (18.0–101.0)		

t: Independent two sample t-test statistics. SD: Standard deviation.

Table 2. Comparison of pelvis type by gender

	Male (n=75)	Female (n=75)	Total (n=150)	Test statistics	p
Pelvis type					
Android	69 (92)	23 (30.7)	92 (61.3)	χ^2=64.333	<0.001
Anthropoid	2 (2.7)	6 (8)	8 (5.3)		
Gynecoid	0 (0)	38 (50.7)	38 (25.3)		
Platypelloid	4 (5.3)	8 (10.7)	12 (8)		

χ^2: Ki-kare test statistics.

Table 3. Comparison of pelvis type according to groups

	Group 1 (n=11)	Group 2 (n=20)	Group 3 (n=119)	Total (n=150)	Test statistics	p
Pelvis type						
Android	0 (0)[a]	0 (0)[a]	92 (77.3)[b]	92 (61.3)	χ^2=83.953	<0.001
Anthropoid	0 (0)	1 (5)	7 (5.9)	8 (5.3)		
Gynecoid	11 (100)[a]	15 (75)[a]	12 (10.1)[b]	38 (25.3)		
Platypelloid	0 (0)	4 (20)	8 (6.7)	12 (8)		

χ^2: Ki-kare test statistics. a-b: There is no difference between groups with the same letter for each pelvis type.

not be created in the superior pubic ramus or the retrograde starting point for the linear corridor was more distal in the parasymphyseal region and had an increased orientation in the caudocranial direction of the sagittal plane in 68.4% of the gynecoid pelvis types. There were statistically significant differences between the distributions of the pelvis types according to the groups (p<0.001) (Table 3).

According to the examination of the CT images obtained from the linear corridor for the superior pubic ramus in group 2, the average corridor width was 3.8±0.8 mm, and the average corridor length was 120.4±7.9 mm. In group 3, the average corridor width was 8.2±1.8 mm, and the average corridor length was 116.7±12.8 mm. In terms of the averages for the entire study (group 2 and group 3 combined), the average corridor width was 7.5±2.3 mm, and the average corridor length was 117.3±12.3 mm. While a statistically significant difference was detected between the groups' corridor width measurements (p<0.001), no statistical difference was found between their length measurements (p>0.001) (Table 4).

The average width of the superior pubic ramus corridor was 8.6±1.6 mm in the android pelvic types, 7.0±2.0 mm in the anthropoid pelvic types, 4.7±1.7 mm in the gynecoid pelvic types, and 5.9±1.8 mm in the platypelloid pelvic types. The average length of the superior pubic ramus corridor was 118.8±7.8 mm in the android pelvic types, 119.2±11.4 mm in the anthropoid pelvic types, 110.6±21.6 mm in the gynecoid pelvic types, and 119.7±8.0 mm in the platypelloid pelvic types.While a difference was detected between corridor diameter values according to pelvis type (p<0.001), no difference was found between length measurements (Table 5).

According to the evaluation of the data based on gender, the average width of the corridor was 9.0±1.4 mm in men and 5.8±1.9 mm in women, and the average length of the corridor was 120.5±7.3 mm in men and 113.6±15.5 mm in women. There was a statistically significant difference between the diameter and length values of the superior pubic arm according to gender (p<0.001) (Table 6).

In the pelvis CT examinations of group 1 and group 2 (n=31), the mean width was 7.7±2.0 mm and the mean length was 89.4±6.1 mm in the medial corridor. The mean width in the lateral aisle was 5.4±1.3 mm, and the mean length in the lateral corridor was 68.8±5.3 mm. There was a statistically significant difference between the diameters of group 1's and group 2's superior pubic ramus in the medial and lateral corridors (Table 7).

To obtain AOO images in the CT images of group 2, an average angle of 48.3±3.9° was required in the coronal plane, and to obtain an inlet image, an average angle of 74.9±4.4° was required in the sagittal plane. In group 3, these angles were 36.4±4.2° for the AOO view and 53.0±5.2° for the inlet view. A statistically significant difference was found between

Table 4. Comparison of superior pubic ramus corridor widths and lengths according to the groups

	Group 2 (n=20)		Group 3 (n=119)		Total (n=139)		Test statistics	p
	Mean±SD	Mean (Min-Max)	Mean±SD	Mean (Min-Max)	Mean±SD	Mean (Min-Max)		
Anterior obdurator outlet width (mm)	4.9±1.1	5.0 (3.0–8.0)	9.1±1.8	9.2 (5.0–13.0)	8.5±2.3	9.0 (3.0–13.0)	t=-13.458	<0.001
Inlet width (mm)	3.8±0.8	3.7 (2.0–6.0)	8.2±1.8	8.2 (4.0–12.0)	7.5±2.3	8.0 (2.0–12.0)	t=-17.646	<0.001
Anterior obdurator outlet length (mm)	120.9±7.9	122.5 (105.0–133.0)	118.3±8.4	118.0 (100.0–138.0)	118.7±8.4	119.0 (100.0–138.0)	t=1.264	0.208
Inlet length (mm)	120.4±7.9	122.2 (104.0–133.0)	116.7±12.8	118.0 (110.0–137.0)	117.3±12.3	118.0 (110.0–137.0)	U=896.0	0.078
Inlet viewing angle (°)	74.9±4.4	74.8 (66.0–84.0)	53.0±5.2	53.0 (40.0–67.0)	56.2±9.2	54.6 (40.0–84.0)	t=17.8	<0.001
Anterior obdurator outlet viewing angle (°)	48.3±3.9	48.0 (42.0–54.0)	36.4±4.2	36.9 (24.0–48.0)	38.1±5.9	37.6 (24.0–54.0)	t=11.77	<0.001

t: Independent two sample t-test statistics; U: Mann-Whitney U test statistics; mm: Millimeter; (°): Degree; SD: Standard deviation.

Table 5. Comparison of superior pubic ramus widths and lengths according to the pelvis type

		Android	Anthropoid	Gynecoid	Platypell	Test statistics	p
Anterior obdurator outlet width (mm)	Mean±SD	9.5±1.6[c]	8.4±1.7[b,c]	5.5±1.7[a]	7.2±1.6[b]	F=44.215	<0.001
	Mean (Min-Max)	9.5 (5.0–13.0)	8.0 (7.0–11.0)	5.2 (3.0–9.0)	6.8 (5.0–10.0)		
Inlet width (mm)	Mean±SD	8.6±1.6	7.0±2.0	4.7±1.7	5.9±1.8	χ^2=61.356	<0.001
	Mean (Min-Max)	9.0 (5.0–12.0)[a]	5.8 (5.0–10.0)[a,b]	4.3 (2.0–8.0)[b]	5.9 (3.0–9.0)[b]		
Anterior obdurator outlet length (mm)	Mean±SD	119.6±7.9	120.0±11.7	114.7±8.3	120.0±8.2	F=2.678	0.050
	Mean (Min-Max)	120.1 (101.0–138.0)	123.0 (100.0–134.0)	115.0 (100.0–130.0)	120.5 (105.0–133.0)		
Inlet length (mm)	Mean±SD	118.8±7.8	119.2±11.4	110.6±21.6	119.7±8.0	χ^2=6.76	0.080
	Mean (Min-Max)	119.4 (101.0–137.0)	123.0 (100.0–132.0)	115.0 (11.0–130.0)	119.0 (107.0–133.0)		
Inlet viewing angle (°)	Mean±SD	52.8±5.0	59.6±9.8	65.3±10.5	58.3±13.3	χ^2=32.596	<0.001
	Mean (Min-Max)	53.0 (40.0–67.0)[a]	59.4 (46.0–79.0)[a,b]	66.0 (46.0–84.0)[b]	56.4 (45.0–77.0)[a,b]		
Anterior obdurator outlet viewing angle (°)	Mean±SD	35.9±4.2c	35.2±5.9[b,c]	43.2±6.5[a]	43.0±5.4[a,b]	F=15.517	<0.001
	Mean (Min-Max)	36.3 (24.0–48.0)	34.3 (28.0–46.0)	42.3 (27.0–54.0)	41.8 (37.0–54.0)		

F: One-way analysis of variance; χ^2: Kruskal Wallis Test Statistics; a-c: There is no difference between types with the same letter; mm: Millimeter; (°): Degree; SD: Standard deviation.

Table 6. Comparison of parameters according to gender

	Male		Female		Test statistics	p
	Mean±SD	Mean (Min-Max)	Mean±SD	Mean (Min-Max)		
Anterior obdurator outlet width (mm)	9.9±1.5	10.0 (5.0–13.0)	6.8±1.8	6.7 (3.0–11.0)	t=11.415	<0.001
Inlet width (mm)	9.0±1.4	9.0 (5.0–12.0)	5.8±1.9	5.6 (2.0–9.0)	t=11.426	<0.001
Anterior obdurator outlet length (mm)	121.2±7.5	122.0 (105.0–138.0)	115.7±8.4	116.0 (100.0–133.0)	t=4.061	<0.001
Inlet length (mm)	120.5±7.3	120.4 (106.0–137.0)	113.6±15.5	114.4 (11.0–133.0)	U=1529.0	<0.001
Inlet viewing angle (°)	52.8±4.5	53.0 (43.0–64.0)	60.2±11.3	57.7 (40.0–84.0)	U=1472.0	<0.001
Anterior obdurator outlet viewing angle (°)	35.4±4.2	35.8 (24.0–48.0)	40.9±6.3	40.4 (27.0–54.0)	t=-6.006	<0.001

t: Independent two sample t-test statistics; U: Mann-Whitney U test statistics; mm: Millimeter; (°): Degree; SD: Standard deviation.

Table 7. Comparison of parameters between group 1 and 2

	Group 1 (n=11)		Group 2 (n=20)		Total (n=31)		Test statistics	p
	Mean±SD	Mean (Min-Max)	Mean±SD	Mean (Min-Max)	Mean±SD	Mean (Min-Max)		
Anterior Obdurator Outlet width (mm) (Medial)	7.7±2.2	7.0 (5.5–12.0)	7.9±2.1	7.8 (4.5–12.0)	7.8±2.1	7.1 (4.5–12.0)	U=98	0.620
Anterior Obdurator Outlet width (mm) (Lateral)	6.1±1.1	6.3 (4.0–7.7)	7.6±1.5	7.3 (5.5–11.0)	7.1±1.5	7.0 (4.0–11.0)	U=42	0.005
Test statistics		Z=-2.535		Z=-0.711				
p		0.011		0.477				
Inlet width (mm) (Medial)	6.7±1.8	6.0 (4.4–10.0)	8.2±2.0	8.0 (4.5–11.9)	7.7±2.0	7.5 (4.4–11.9)	t=2.142	0.041
Inlet width (mm) (Lateral)	4.3±1.1	4.0 (2.6–6.2)	6.0±1.0	6.4 (3.5–7.5)	5.4±1.3	5.5 (2.6–7.5)	t=4.38	<0.001
Test statistics*	t=-4.588	t=-4.302						
p	<0.001	<0.001						
Anterior obdurator outlet length (mm) (Medial)	89.2±6.8	88.0 (78.0–100.0)	89.5±6.0	89.5 (80.0–106.0)	89.4±6.1	89.0 (78.0–106.0)	t=0.11	0.913
Anterior obdurator outlet length (mm) (Lateral)	69.6±4.6	69.5 (64.0–79.0)	68.3±5.7	66.5 (59.0–77.5)	68.8±5.3	68.0 (59.0–79.0)	t=-0.646	0.523
Test statistics*		t=-7.803		t=-13.676				
p		<0.001		<0.001				
Inlet length (mm) (Medial)	89.3±6.5	89.0 (79.0–99.0)	89.6±5.9	89.0 (80.0–106.0)	89.5±6.0	89.0 (79.0–106.0)	U=106	0.868
Inlet length (mm) (Lateral)	69.9±4.6	70.0 (65.0–80.0)	68.4±5.6	66.5 (60.0–77.5)	68.9±5.2	67.0 (60.0–80.0)	U=82	0.245
Test statistics		Z=-2.936		Z=-3.922				
p		0.003		<0.001				

t: Independent two sample t-test statistics; *t: Paired two sample t-test statistics; U: Mann-Whitney U test statistics; Z: Wilcoxon test statistics; mm: Millimeter; SD: Standard deviation.

the angle values required to obtain inlet and AOO images ($p<0.001$) (Table 4). To create a corridor, the angular values required in the coronal and sagittal planes were compared to the pelvis types, lower angle values were required in the android pelvis type, and higher angle values were required in the gynecoid pelvis type (Table 5). For the evaluation made according to gender, lower angle values for the coronal and sagittal planes were required in men than in women (Table 6). There was a statistically significant difference between the angle values required to obtain inlet and AOO images according to gender and pelvic type ($p<0.001$).

DISCUSSION

Due to the complex and three-dimensional anatomical structure of the pelvis, the surgical evolution of this region is slow when compared to other anatomical regions. Nonetheless, it has gained momentum due to recent developments in imaging and surgical techniques. Over the last 50–60 years, cornerstones in the surgical evolution for pelvis-acetabulum fractures have included Judet et al.'s[24] classification of acetabular fractures and description of surgical approaches, Matta et al.'s[25,26] impactful results of open reduction and internal fixation for acetabulum fractures, and Routt et al.'s[11,27] studies on percutaneous screw fixation. The retrograde screw fixation technique, which Routt et al.[12] defined a quarter of a century ago as a new method for fixation superior pubic ramus fractures, has provided positive developments and advancements in surgery and imaging. In this context, bone fixation pathways have been described for pelvic and acetabular fracture surgeries.[8,12,20,28]

In studies of the superior pubic ramus and acetabulum anterior column, in addition to studies reporting opposite opinions, screw placement errors, or gender-specific differences, linear corridors have been detected in all patients.[10–16,18–20] For superior pubic ramus fractures, the failure to detect a linear corridor extending to the supraacetabular region in a retrograde fixation has led to the idea that pelvis type may be effective for obtaining a long linear corridor. In our study, no linear corridor for the superior pubic arm could be obtained from group 1's (7.3%) CTs in any way. In group 2 (13.3%), the corridor diameter was below 5 mm. Although studies have examined the differences between the acetabulum anterior columns of males and females, we could not find any study investigating whether pelvis type affects the fixation of the superior pubic ramus.[14,16] In group 1 of the present study, the pelvis type was gynecoid in all CT images, no linear corridor could be obtained, and all the patients were female. In group 2, the gynecoid pelvis type was dominant. For the android pelvis type, a linear corridor could easily be created in the retrograde superior pubic ramus of both men and women.

According to the literature review, although there is no clear consensus, there are anatomical, clinical, and radiological studies on the diameter of the superior pubic ramus and corridor length. In addition, clinical studies have suggested 3.5/4.5 mm screws for fixation,[12] and anatomical and radiological studies have indicated that corridor width is more than 10 mm on average.[11,17] In the current study, the diameter of the superior pubic ramus for group 2 was 3.8±0.8 mm, which is consistent with recommendations from Rout et al.'s[12] research. Moreover, the diameter of the superior pubic ramus was 8.2±1.8 mm for group 3 and 7.5±2.3 mm for groups 2 and 3 combined, which is compatible with findings from the literature.[12,13,15,18,20,28] Similar to the literature, the results of the present study revealed that the corridor diameter values were significantly higher in males than in females.[11,14,16,29]

Furthermore, in radiological corridor studies of the acetabulum anterior arm that examined the differences between male and female genders, it was determined that the corridor diameter in CT images of men was statistically longer than the corridor diameter in CT images of women.[11,14,16] In the current study's evaluation of the superior pubic ramus diameters according to pelvis type, diameter measurements were higher in pelvic CT images of the android pelvis type, and the predominant pelvis type was android in the male patient group. These results are consistent with the literature.

The length of the superior pubic ramus corridor has ranged from 103 mm to 173.2 mm in studies from the literature.[11,13,14,16–19] The reason for the wide range of corridor length measurements may be due to differences in gender, age, height, weight, race, and pelvis type. The average corridor length in our study was 117.3±12.3 mm, which is consistent with results from the literature.

The medial and lateral corridor diameters in the CT images for groups 1 and 2 were similar to those produced in Quan et al.'s[13] radiographic simulation study of retrograde screw insertion into the superior pubic ramus. In examinations where a linear corridor or corridor smaller than 5 mm cannot be created, which constituted 20.7% of our study sample, medial or lateral corridors may be used since a long screw cannot be used for superior pubic ramus fractures due to the localization of the fracture. This strategy also coincides with retrograde fixation recommendations for Nakatani type 1 and 2 fractures and antegrade screw fixation recommendations for type 3 fractures.[9]

To create a corridor for the superior pubic ramus, angles of 38.1±5.9° and 56.2±9.2° were required in the coronal and sagittal planes, respectively. When evaluating according to gender and pelvis type to obtain images in the coronal and sagittal planes of females with gynecoid pelvis types, larger angle values were required. Our data differed from values in radiological studies from the literature.[11,14] We believe this is due to differences in gender, age, height, weight, race, and pelvis type among the studies.

Some studies have reported frequent screw insertion failure, screw separation, loss of reduction, and return of screws in

female patients.[12,20] Moreover, anatomical[10] and radiological studies[11,14,18,29] have shown that women do not always have a long, thick screw corridor for fixation of the acetabulum anterior column. Our study's findings can be summarized as follows: 1) all pelvis types in group 1, which could not form linear corridors, had gynecoid characteristics; 2) gynecoid pelvis types that were less than 5 mm in diameter were predominantly found in group 2; 3) linear corridors could be formed in the retrograde superior pubic ramus of both male and female patients with the android pelvis type; and 4) frequent observation of the android pelvis type in the male population strongly supported our hypothesis.

Limitations

This study is a radiological study and should be supported by anatomical studies. In addition, developments in imaging and measurement techniques, together with developing technology, may affect measurement results. Some pelvis structures do not precisely fit the four main pelvis groups, and they were included in the main pelvis group closest to them. This is another negative aspect of our study. Results are valid only for individuals aged 16–100 years. In addition, our study reflects our assumptions limited to a sample group of a particular region and race. Therefore, the generalizability of the study is limited.

Conclusion

For percutaneous detection of the superior pubic ramus, no linear corridor could be comfortably obtained in all patients. These circumstances are especially difficult for women and patients with a gynecoid pelvic type. The male gender and android pelvis type can be advantageous for percutaneous fixation in a long and wide corridor. The pelvis typing with MPR and the 3D modeling mode of CT examination during preoperative planning may shed light on various factors, such as surgical planning, implant selection, and surgical position.

Ethics Committee Approval: This study was approved by the Samsun Training and Research Hospital Non-interventional Clinical Research Ethics Committee (Date: 09.12.2020, Decision No: 2020/16/10).

Peer-review: Externally peer-reviewed.

Authorship Contributions: Concept: H.A., O.B.; Design: H.A., O.B.; Supervision: H.A., O.B.; Resource: H.A., O.B.; Materials: H.A., O.B.; Analysis: H.A., O.B.; Literature search: H.A., O.B.; Writing: H.A., O.B.; Critical revision: H.A., O.B.

Conflict of Interest: None declared.

Financial Disclosure: The authors declared that this study has received no financial support.

REFERENCES

1. Melhem E, Riouallon G, Habboubi K, Gabbas M, Jouffroy P. Epidemiology of pelvic and acetabular fractures in France. Orthop Traumatol Surg Res 2020;106:831–9.
2. Rinne PP, Laitinen MK, Huttunen T, Kannus P, Mattila VM. The incidence and trauma mechanisms of acetabular fractures: a nationwide study in Finland between 1997 and 2014. Injury 2017;48:2157-61.
3. Kannus P, Parkkari J, Niemi S, Sievänen Het. Low-trauma pelvic fractures in elderly Finns in 1970-2013. Calcif Tissue Int 2015;97:577–80.
4. Routt Jr ML, Kregor PJ, Simonian PT, Mayo KA. Early results of percutaneous iliosacral screws placed with the patient in the supine position. J Orthop Trauma 1995;9:207–14.
5. Giannoudis PV, Tzioupis CC, Pape HC, Roberts CS. Percutaneous fixation of the pelvic ring: an update. J Bone Joint Surg Br 2007;89:145–4.
6. Starr AJ, Walter JC, Harris RW, Reinert CM, Jones AL. Percutaneous screw fixation of fractures of the iliac wing and fracture-dislocations of the sacro-iliac joint (OTA Types 61-B2.2 and 61-B2.3, or Young-Burgess "lateral compression type II" pelvic fractures). J Orthop Trauma 2002;16:116–23.
7. Barei DP, Shafer BL, Beingessner DM, Gardner MJ, Nork SE, Routt MC. The impact of open reduction internal fixation on acute pain management in unstable pelvic ring injuries. J Trauma 2010;68:949–53.
8. Bishop JA, Routt ML Jr. Osseous fixation pathways in pelvic and acetabular fracture surgery: osteology, radiology, and clinical applications. J Trauma Acute Care Surg 2012;72:1502–9.
9. Starr AJ, Nakatani T, Reinert CM, Cederberg K. Superior pubic ramus fractures fixed with percutaneous screws: what predicts fixation failure? J Orthop Trauma 2008;22:81–7.
10. Ebraheim NA, Xu R, Biyani A, Benedetti JA. Anatomic basis of lag screw placement in the anterior column of the acetabulum. Clin Orthop Relat Res 1997;339:200–5.
11. Suzuki T, Soma K, Shindo M, Minehara H, Itoman M. Anatomic study for pubic medullary screw insertion. J Orthop Surg 2008;16:321–5.
12. Routt Jr ML, Simonian PT, Grujic L. The retrograde medullary superior pubic ramus screw for the treatment of anterior pelvic ring disruptions: a new technique. J Orthop Trauma 1995;9:35–44.
13. Quan Q, Hong L, Chang B, Liu RX, Zhang YQ, Zhao Q, et al. A radiographic simulation study of fixed superior pubis ramus fractures with retrograde screw insertion. J Orthop 2016;13:364–8.
14. Chen KN, Wang G, Cao LG, Zhang MC. Differences of percutaneous retrograde screw fixation of anterior column acetabular fractures between male and female: a study of 164 virtual three- dimensional models. Injury 2009;40:1067–72.
15. Grossterlinden L, Nuechtern J, Begemann PG, Fuhrhop I, Petersen JP, Ruecker A, et al. Computer-assisted surgery and intraoperative three--dimensional imaging for screw placement in different pelvic regions. J Trauma 2011;71:926–32.
16. Gras F, Gottschling H, Schroder M, Marintschev I, Reimers N, Burgkart R. Sex-specific differences of the infraacetabular corridor: a biomorphometric CT-based analysis on a database of 523 pelves. Clin Orthop Relat Res 2015;473:361–9.
17. Shahulhameed A, Roberts CS, Pomeroy CL, Acland RD, Giannoudis PV. Mapping the columns of the acetabulum implications for percutaneous fixation. Injury 2010;41:339–42.
18. Attias N, Lindsey RW, Starr A, Borer D, Bridges K, Hipp JA. The use of a virtual three-dimensional model to evaluate the intraosseous space available for percutaneous screw fixation of acetabular fractures. J Bone Joint Surg Br 2005;87:1520–3.
19. Chen H, Tang P, Yao Y, She F, Wang Y. Anatomical study of anterior column screw tunnels through virtual three-dimensional models of the pelvis. Eur J Orthop Surg Traumatol 2015;25:105–10.
20. Starr AJ, Reinert CM, Jones AL. Percutaneous fixation of the columns of

the acetabulum: a new technique. J Orthop Trauma 1998;12:51–8.
21. Caldwell WE, Moloy HC. Anatomical variations in the female pelvis: their classification and obstetrical significance. Proc R Soc Med 1938;32:1–30.
22. Lenhard M, Johnson T, Weckbach S, Nikolaou K, Friese K, Hasbargen U. Three-dimensional pelvimetry by computed tomography. Radiol Med 2009;114:827–34.
23. Salk I, Cetin A, Salk S, Cetin M. Pelvimetry by three-dimensional computed tomography in non-pregnant multiparous women who delivered vaginally. Pol J Radiol 2016;81:219–27.
24. Judet R, Judet J, Letournel E. Fractures of the acetabulum classification and surgical approaches for open reduction. J Bone J Surg 1964;46:1615–46.
25. Matta M, Anderson LM, Epstein HC. Fractures of acetabulum: a retrospective analysis. Clin Orthop 1986;205:230–40.
26. Matta M, Mehne DK, Roffi R. Fractures of acetabulum: early results of a prospective study. Clin Orthop 1986;205:241–50.
27. Routt Jr ML, Simonian PT. Internal fixation of pelvic ring disruptions. Injury 1996;27:20–30.
28. Routt Jr ML, Nork SE, Mills WJ. Percutaneous fixation of pelvic ring disruptions. Clin Orthop 2000;375:15–29.
29. Puchwein P, Enninghorst N, Sisak K, Ortner T, Schildhauer TA, Balogh ZJ, et al. Percutaneous fixation of acetabular fractures: computer-assisted determination of safe zones, angles and lengths for screw insertion. Arch Orthop Trauma Surg 2012;132:805–11.

ORİJİNAL ÇALIŞMA - *ÖZ*

Pelvis tipi perkütan pubik ramus tespitinde etkili midir?

Dr. Harun Altınayak,[1] Dr. Orhan Balta[2]

[1]Samsun Eğitim ve Araştırma Hastanesi, Ortopedi ve Travmatoloji Kliniği, Samsun
[2]Tokat Gaziosmanpaşa Üniversitesi Tıp Fakültesi, Ortopedi ve Travmatoloji Kliniği, Tokat

AMAÇ: Pelvis tipinin, perkütan superior pubik ramus tespitine etkisini araştırmak amaçlanmıştır.
GEREÇ VE YÖNTEM: Pelviste anatomik değişikliği olmayan 150 pelvis BT(kadın/erkek: 75/75) üzerinde çalışıldı. 1 mm kesit genişliğinde çekilen pelvis BT tetkikleri, görüntüleme sisteminin MPR ve 3D görüntüleme modu kullanılarak; pelvis tiplendirilmesi, anterior obturator oblik ve inlet kesit görüntüleri oluşturuldu. Bu görüntülerde superior pubik ramus için doğrusal bir koridor elde edilip edilemediği, doğrusal koridor elde edilebilen pelvis BT'lerinde koridor genişliği, uzunluğu ile transvers ve sagittal düzlemdeki açı değerleri ölçüldü.
BULGULAR: Örneklemin 11'inde (%7.3) (grup1) herhangi bir şekilde superior pubik ramus için doğrusal bir koridor elde edilemedi. Bu gruptaki tüm pelvis tipleri gynecoid özellikte idi ve hepsi kadın hastalara aitti. Android pelvis tipine sahip tüm pelvis BT'lerinde rahatlıkla superior pubik ramusta doğrusal bir koridor elde edilebilmekteydi. Süperior pubik ramus genişliği ortalama 8.2±1.8 mm, uzunluğu ortalama 116.7±12.8 mm idi. Yirmi (%13.3) pelvis BT görüntüsünde (grup 2) koridor genişliği 5 mm altında ölçüldü. Koridor genişliği, pelvis tipine ve cinsiyete bağlı istatiksel olarak anlamlı farklılık arz etmekteydi.
TARTIŞMA: Pelvis tipi perkutan superior pubik ramus tespitinde etkili bir faktördür. Bu sebeple preoperatif BT tetkikinde MPR ve 3D görüntüleme modu kullanılarak yapılacak pelvis tiplendirmesi; cerrahi plan, implant ve cerrahi pozisyon seçiminde etkilidir.
Anahtar sözcükler: 3D görüntüleme; MPR; pelvis BT; perkütan vida fiksasyonu; süperior pubik kol.

Ulus Travma Acil Cerrahi Derg 2023;29(3):419-429 doi: 10.14744/tjtes.2023.54545